The Canadian Journal of Mineralogy and Petrology
ISSN 2817-1713
Vol. 63, pp. 867-878 (2025)
DOI: 10.3749/250007

TOURETITE, $LiAl_4Be_4(B_{11}Be)O_{28}$, A NEW BORATE MINERAL FROM THE AMBALABE PEGMATITE, MADAGASCAR

Frédéric HATERT[§], Martin DEPRET, and Florent BOMAL

Laboratoire de Minéralogie, Département de Géologie, Université de Liège, Bâtiment B18, Sart Tilman, B-4000 Liège, Belgique

Federico PEZZOTTA

MUM – Mineralogical Museum "Luigi Celleri", San Piero in Campo, Elba Island, Italy

Pietro VIGNOLA

CNR-Istituto di Geologia Ambientale e Geoingegneria – via Mario Bianco, 9 - 20131 Milano, Italia

Markus WÄLLE and Pierre LEFÈVRE

Swiss Gemmological Institute SSEF, Aeschengraben 26, 4051 Basel, Switzerland

Radek ŠKODA

Department of Geological Sciences, Masaryk University, Kotlářská 267/2, 611 37 Brno, Czech Republic

Anatoly V. KASATKIN and Atali A. AGAKHANOV

Fersman Mineralogical Museum of the Russian Academy of Sciences, Leninsky Prospect 18-2, 119071 Moscow, Russia

Natalia V. ZUBKOVA

Faculty of Geology, Moscow State University, Vorobievy Gory, 119991 Moscow, Russia

Mattia BONAZZI and Alberto ZANETTI

CNR-Centro di Studio per la Cristallochimica e la Cristallografia, Strada Ferrata 1, I-27100 Pavia, Italia

Nicola ROTIROTI and Andrea RISPLENDENTE

Dipartimento di Scienze della Terra, Università degli Studi di Milano - via Botticelli 23, I-20133 Milano, Italy

Abstract

Touretite, $LiAl_4Be_4(B_{11}Be)O_{28}$, is a borate mineral found in the Ambalabe granitic pegmatite, Madagascar. The mineral, which is the Li-rich analogue of londonite and rhodizite, occurs as white to pinkish rhombic-dodecahedral crystals reaching 1 cm in diameter and is deposited on tourmalines, feldspars, and heavily corroded spodumene and danburite. The streak is white, the luster vitreous, and touretite does not show any fluorescence under short wave (254 nm) or long wave (366 nm) ultraviolet light. The Mohs hardness is 8, cleavage is absent, the tenacity is brittle, the fracture is conchoidal, and the measured density is 3.06(1) g/cm^3. Optically, touretite is colorless, isotropic, non-pleochroic, and shows an index of refraction of $n = 1.6952 \pm 0.0005$ (measured using a light source of 589 nm wavelength). The empirical formula, calculated on the basis of 28 oxygen atoms per formula unit from the chemical analysis determined by LA-TOF-ICP-MS, is $(Li_{0.38}Cs_{0.24}K_{0.14}Rb_{0.03}Na_{0.02}Pb_{0.01}\square_{0.18})_{\Sigma 1.00}(Al_{4.00}Si_{0.05}Fe^{2+}_{0.03}Mn_{0.02})_{\Sigma 4.10}(Be_{3.60}Li_{0.40})_{\Sigma 4.00}(B_{11.28}Be_{0.72})_{\Sigma 12.00}O_{28}$. The cubic unit-cell parameters, determined by single-crystal X-ray diffraction

§ *Corresponding author e-mail address*: fhatert@uliege.be

methods, are $a = 7.31202(15)$ Å, V = 390.942(14) Å^3. The structure refinement was performed in space group $P\bar{4}3m$ from 226 unique reflections to the final R_1 value of 0.0444. The structure of touretite contains clusters of four edge-sharing AlO_6 octahedra located around the origin of the unit cell and linked to the BeO_4 and BO_4 tetrahedra by corner-sharing. The alkali cations occupy the Li/Cs site in a large cavity at the center of the unit cell and have a coordination number of 12. The coordination polyhedron can be described as a truncated tetrahedron that shares its small triangular faces with faces of the BeO_4 tetrahedra. The species was accepted by the IMA-CNMNC under number IMA 2023-003a, and the name was chosen to honor Jacques and Lydie Touret, for their contribution to mineralogical sciences.

Keywords: touretite, borate, rhodizite-londonite group, granitic pegmatites, Madagascar.

Introduction

Minerals of the rhodizite-londonite series are rare borates occurring in some LCT granitic pegmatites in Madagascar, Russia, the USA, and the UK. Rhodizite, the potassic endmember, was first described by Rose (1834) on tourmaline crystals from the Ural mountains, stored in the Royal Museum of Berlin mineral collection. The rhombic-dodecahedral shape of the crystals, as well as preliminary chemical tests, allowed Rose (1834) to confirm the new species and to underline some similarities with boracite. The quantitative chemical data obtained by Damour (1882) on Russian samples did not allow the determination of alkalis and of the light elements Be and Li; however, the investigation of new rhodizite samples from Madagascar (Lacroix 1922) led to a better characterization of the chemical composition of the species. As noted by Simmons *et al.* (2001) and Pekov *et al*. (2010), who described in detail the history of those minerals, the first charge-balanced formula of rhodizite was determined by Pring *et al.* (1986), by merging all available chemical and structural data. The simplified formula for rhodizite given by these authors is $(K,Cs)Al_4Be_4(B,Be)_{12}O_{28}$, leading to the endmember formula $KAl_4Be_4(B_{11}Be)O_{28}$. Londonite, the Cs-dominant analogue of rhodizite, was described from the Antandrokomby pegmatite, Madagascar, by Simmons *et al*. (2001).

Recent studies by Gatta *et al.* (2010) confirm that londonite from Madagascar is anhydrous, and that the tetrahedral sites in the structure show a partially disordered distribution of Be and B. The stability of this species at high pressures and temperatures was investigated by Gatta *et al.* (2011), who consider londonite to be a potential neutron absorbing material. By using historical samples from the Urals, Russia, Pekov *et al*. (2010) also collected crystal-chemical data on londonite, showing the existence of complex heterovalent substitutions and of a hypothetical endmember with vacancies dominant on the large alkalis site.

Laurs *et al*. (2002) investigated gem-quality samples in the rhodizite–londonite solid solution series from the Antsongombato pegmatite in Madagascar in order to characterize their gemological properties, such as fluorescence, refraction indices, and the presence of inclusions. They also obtained infrared and UV-visible spectral data and determined the chemical compositions of eight treated and untreated samples by electron microprobe and X-ray fluorescence spectrometry. These last techniques, however, did not allow the determination of light elements such as Be, B, and Li, which are of major importance in rhodizite-type minerals.

Most rhodizite–londonite samples are colorless, yellow, or greenish, but recent finds in Madagascar provided samples with unusual orange, pink, gray, black, or brown colors; 32 of these were crystal-chemically investigated by Totaro (2021). The structural data, coupled with laser ablation time-of-flight inductively-coupled-plasma mass spectrometry (LA-TOF-ICP-MS, abbreviated GemTOF), indicated that Fe and Mn are responsible for the orange and yellow colors, and that Cr may be responsible for the green colors. A pink crystal showed an enrichment in manganese (15 ppm Mn) and in lithium (3000 ppm Li), as well as high amounts of vacancies reaching 0.37 □ per formula unit (*pfu*). This composition clearly approaches the vacant-dominant endmember previously suggested by Pekov *et al*. (2010).

Similar samples of "pink londonites" were investigated in 2019 by the Hatert-Pezzotta-Vignola research team (acronym HPV), who submitted a proposal to the CNMNC under the name "touretite", in January 2023 (IMA # 2023-003). Light elements in this mineral were measured by excimer laser ablation inductively-coupled-plasma mass spectrometry (ELA-ICP-MS), and the poor resulting data gave an unrealistic empirical formula with an excess of aluminum on the octahedral site of the structure, thus leading to the vacancy-dominant $□Al_4Be_4B_{12}BeO_{28}$ endmember formula. The mineral was rejected by the CNMNC due those chemical inconsistencies, but the new analytical data obtained recently by GemTOF at the Schweizerische Stiftung für Edelstein-Forschung (SSEF), Basel, confirmed the presence of lithium substituting for the large alkalis in the structure. In parallel, a similar sample from the same locality was investigated by the Agakhanov-Kasatkin-Nestola-Škoda-Zubkova research team (acronym AKNŠZ), leading to another set of independent analytical data, including electron-probe microanalyses

(EPMA), laser ablation inductively-coupled-plasma mass spectrometry (LA-ICP-MS), single-crystal X-ray diffraction data (SCXRD), and optical measurements. After merging both research teams, the touretite proposal was revisited using GemTOF, EPMA, and SCXRD data from the HPV team and some optical data from the AKNŠZ team; it was finally accepted by the CNMNC under number IMA 2023-003a. The species is the lithium-dominant endmember of the rhodizite group, with the $LiAl_4Be_4(B_{11}Be)O_{28}$ endmember formula. Its mineral symbol is "Tte", according to the system defined by Warr (2021).

The name touretite was chosen to honor Jacques and Lydie Touret, for their contribution to mineralogical sciences. Jacques was mineralogy, petrography, and metallogeny professor at the University Paris-Diderot during the period 1972–1980, and then at the University of Amsterdam from 1980 to his retirement in 2001. He was particularly renowned for his studies on fluid inclusions and on rock-forming minerals, with a particular attention to granulitic metamorphic rocks. Jacques continued his scientific activities by publishing and participating in conferences, until he sadly passed away on March 11th, 2024. Lydie, his wife, was mineralogy curator at the Mineralogy Museum of the École des Mines Paris-Tech, during the period 1992–2012. Under her direction, the mineralogy collections were significantly improved with a number of donations and purchases, thanks in part to a close collaboration with the association "Les Amis de la Bibliothèque et de l'École des Mines". Lydie served as Chairwoman of the International Mineralogical Association – Commission on Museums (IMA-CM) during the period 2008–2013.

The holotype samples used for the complete characterization of touretite are deposited in the Mineralogical Collection of the Laboratoire de Minéralogie, University of Liège, Belgium (sample used for optical measurements, X-ray powder diffraction, and GemTOF analyses, catalog number ULG-21979) and in the Mineralogical Collection of the Museo Civico di Storia Naturale di Milano, Italy (sample used for EMPA and SCXRD, catalog number M39042). The samples investigated by the AKNŠZ research team, used to complete our chemical and optical characterization, are considered as cotypes and are stored in the Fersman Museum in Moscow, catalog number 98810.

Occurrence

Touretite was found in the Ambalabe Pegmatite, located at 25 km south of Antsirabe, Betafo mining district, central Madagascar (20° 14' 25" S, 47° 1' 18"E). The pegmatite is constituted by several dikes with thicknesses from a few centimeters to over two meters, hosted in dolomitic marbles of the metamorphic Itremo Group (Pezzotta 2005). An extreme enrichment in boron, characteristic for the region, produced several rare species, for example danburite, tourmaline-group minerals, and rhodizite-group minerals (Pezzotta 2005). According to Pezzotta (2001), such pegmatites correspond to a new "Danburite subtype" of the Rare-Element pegmatite class (Černý & Ercit 2005).

Fig. 1. Whitish to pale pink rhombic-dodecahedral crystal of touretite measuring 13 mm in diameter, from the holotype n° M39042.

The area is well known for pegmatites mined for gemstones, such as tourmaline gem varieties, morganite, kunzite, spessartine, and danburite. The Ambalabe pegmatite was mostly mined for mineral specimens and, in particular, tourmaline and associated minerals. In the core zone of the body, touretite was found in many rhombic-dodecahedral crystals formed at a late-stage and deposited on tourmalines, feldspars, and heavily corroded spodumene and danburite. Touretite formed together with a late-stage generation of sugary-white to very pale blue albite and milky quartz overgrowing pre-existing large crystals or as a new generation of small crystals. Locally, a pearly white phyllosilicate occurring as small blades (unstudied) is also found in association with touretite.

The complete list of mineral species associated with touretite includes quartz, albite, microcline, tourmaline-group minerals (dravite, schorl, elbaite, fluor-liddicoatite), spodumene, "lepidolite", danburite, columbite-(Mn), fersmite, pyrochlore-supergroup minerals (not studied so far), and bismuthinite.

Physical and Optical Properties

Touretite forms large crystals up to 1 cm in diameter (Fig. 1), characterized by the dominant {110} rhombic dodecahedron sometimes associated with the less developed {111} and $\{\bar{1}11\}$ tetrahedral faces. The color is milky white, creamy white to pale pink, or pink, and interpenetration twins, as well as

TABLE 1. CHEMICAL DATA FOR TOURETITE

Constituent	Mean (wt.%)	Range (wt.%)	Standard deviation	Cation numbers per formula unit
B_2O_3	52.11	51.25–53.21	0.88	11.281
BeO	14.35	13.77–14.80	0.41	4.323
Al_2O_3	27.04	26.67–27.33	0.05	3.997
SiO_2	0.37	0.22–0.46	0.10	0.047
FeO	0.29	0.26–0.32	0.03	0.030
MnO	0.21	0.18–0.23	0.02	0.022
PbO	0.27	0.09–0.49	0.19	0.009
Li_2O	1.54	1.37–1.70	0.13	0.776
Na_2O	0.08	0.06–0.10	0.02	0.019
K_2O	0.90	0.41–1.25	0.39	0.144
Rb_2O	0.40	0.19–0.55	0.16	0.032
Cs_2O	4.53	3.43–5.67	0.89	0.242
Total	102.06			

polysynthetic twins, were observed. The streak is white, the luster vitreous, and touretite does not show fluorescence under short wave (254 nm) or long wave (366 nm) ultraviolet light.

The Mohs hardness is 8, according to a direct determination by quartz and corundum scratch tests. Cleavage is absent, the tenacity is brittle, and the fracture is conchoidal. The density, measured by immersion in Clerici solutions, is 3.06(1) g/cm^3, in fairly good agreement with the values obtained from the single-crystal structure refinement (3.19 g/cm^3) and from the single-crystal unit-cell parameters coupled with GemTOF data (3.266 g/cm^3).

Optically, touretite is colorless, isotropic, and shows an index of refraction of $n = 1.6952 \pm 0.0005$, measured by immersion in index of refraction liquids, with a polarizing microscope using a light source of 589 nm wavelength. The mineral is non-pleochroic.

Chemical Composition

Chemical analyses of touretite were performed with the LA-ICP-TOF-MS (GemTOF) spectrometer located at the SSEF, Basel, Switzerland. The instrument is constituted by a laser ArF of 193 nm wavelength, coupled with a ICP-TOF-MS icpTOF (TOFWERK AG, Switzerland). The ICP power is between 1300 and 1350 W, and the instrument measures a complete mass spectrum from $^7Li^+$ to $^{238}U^+$, thus allowing the determination of all elements of the periodic table, except hydrogen and elements heavier than uranium.

The results of five GemTOF analyses performed on five grains of touretite are reported in Table 1. Conditions used for the ablation were 75 μm crater diameter, repetition rate 22 Hz, fluence 5.6 J/cm^2. The carrier gas was He, with a flow rate of 0.8–0.9 L/min. Five He purges were conducted before the measurements, with an ablation time of 30 s each, and the quantification was done with a MATLAB script developed at the SSEF (Wang & Krzemnicki 2021). Standard materials used were the glasses NIST610 and NIST612. The final data were normalized to the Al content previously determined with a Jeol JXA-8200 WDS electron microprobe (University of Milan, 15 kV, 5 nA, beam diameter 5 μm). The standard used was anorthite (An 137), and the resulting Al content was 27.04 wt.% Al_2O_3 (based on the average of eight point analyses).

The empirical formula of touretite, calculated on the basis of 28 oxygen atoms per formula unit, is $(Li_{0.38}Cs_{0.24}K_{0.14}Rb_{0.03}Na_{0.02}Pb_{0.01}\square_{0.18})_{\Sigma 1.00}(Al_{4.00}Si_{0.05}Fe^{2+}_{0.03}Mn_{0.02})_{\Sigma 4.10}(Be_{3.60}Li_{0.40})_{\Sigma 4.00}(B_{11.28}Be_{0.72})_{\Sigma 12.00}O_{28}$. The simplified formula is $(Li,Cs,K)Al_4(Be,Li)_4(B,Be)_{12}O_{28}$, and the ideal formula is $LiAl_4Be_4(B_{11}Be)O_{28}$, which requires Al_2O_3 28.06, BeO 17.21, B_2O_3 52.68, Li_2O 2.06, total 100 wt.%.

The compatibility index, according to Mandarino (1981), is $1 - (K_P/K_C) = -0.0009$, Superior (calculated from the density 3.266 g/cm^3 obtained from SC-XRD unit-cell parameters and Gem TOF analyses).

Raman and Infrared Spectroscopy

The Raman spectrum of touretite (Fig. 2) was obtained with a Horiba Labram HR Evolution spectrometer. This dispersive, edge-filter-based system is equipped with an Olympus BX 41 optical microscope, a diffraction grating with 600 grooves per millimeter, and a Peltier-cooled, Si-based charge-coupled device (CCD) detector. The Raman signal was excited by a 532 nm laser. The nominal laser beam energy of 50 mW was attenuated to 25% using a neutral density filter to avoid the thermal damage to the analyzed area. The Raman signal was collected in the range of 50–4000 cm^{-1} with a 100× objective and the system being operated in the confocal mode, beam diameter

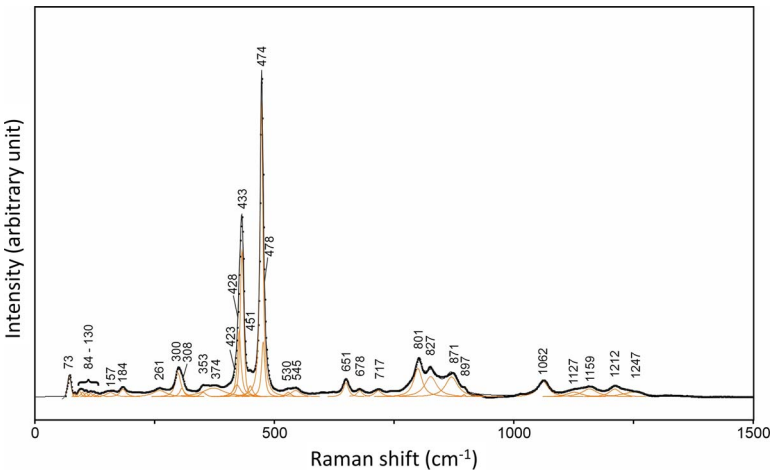

FIG. 2. The Raman spectrum of touretite excited by a 532 nm laser in the 60–1500 cm^{-1} region. The measured spectrum is shown by dots. The curve matching to dots is a result of spectral fit as a sum of individual Voigt peaks (orange) shown below the curve.

was ~2.6 μm and the axial resolution ~5 μm. Time acquisition was 120 s per spectral window; five accumulations and seven spectral windows were applied to cover the 60–4000 cm^{-1} range. Wavenumber calibration was done using the Rayleigh line and low-pressure Ne-lamp emissions. The wavenumber accuracy was ~0.5 cm^{-1}, and the spectral resolution was ~2 cm^{-1}. Band fitting was done after appropriate background correction, assuming combined Lorentzian-Gaussian band shapes using Voight function (*PeakFit*; Jandel Scientific Software). No Raman bands were observed above 1250 cm^{-1}; an intensive luminescence is present in the 2800–4000 cm^{-1} region.

The Raman spectrum of touretite (Fig. 2) is similar to the spectrum of rhodizite published by Frost *et al.* (2014). The observed Raman bands were assigned according to publications of Ross (1972), Hofmeister *et al.* (1987), Kim *et al.* (1995), and Frost *et al.* (2014). Raman scattering in the 1100–1250 cm^{-1} range corresponds to antisymmetric stretching vibrations of B–O units, and the Raman band at 1062 cm^{-1} is assigned to symmetric stretching vibrations of B–O units. The bands in the 800–900 cm^{-1} region are assigned to O–B–O and O–Be–O bending vibrations, and the bands in the 650–720 cm^{-1} range are interpreted as stretching modes of Be–O bonds overlapping with B–O vibrations. The Al–O stretching vibrations are present in the 400–500 cm^{-1} region.

The Fourier-transform infrared (FTIR) spectrum of touretite (Fig. 3) was recorded by the attenuated total

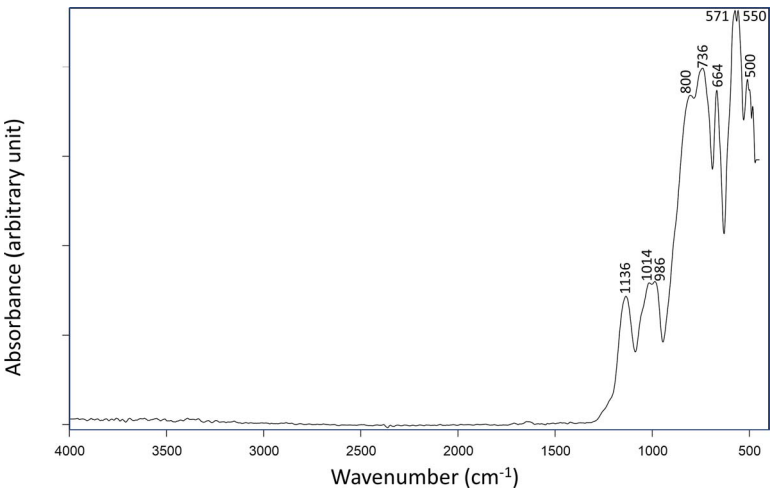

FIG. 3. The infrared spectrum of touretite.

reflection (ATR) method with a Ge crystal on a LUMOS II (Bruker) micro spectrometer. The spectrum was collected over the wavenumber range from 4000 to 450 cm^{-1} using LN2 cooled MCT detector. The spectrum was obtained by the co-addition of 200 scans (to improve signal-to-noise ratio) with a resolution of 2 cm^{-1} and from the area 100 × 100 μm delimited by knife-edge apertures. Band fitting was done after appropriate background correction, assuming combined Lorentzian-Gaussian band shapes using the Voight function (*PeakFit*; Jandel Scientific Software).

Bands in the infrared spectrum of touretite (Fig. 3) were assigned according to Pekov *et al*. (2010) and Frost *et al*. (2014). The absence of significant bands around 3500 and 1600 cm^{-1} confirms the absence of water molecules and OH groups in touretite, while Pekov *et al.* (2010) observe small amounts of H_2O molecules in two londonite samples, and small amounts of OH groups in one rhodizite sample. The antisymmetric stretching vibrations of the BO_4 tetrahedra produce the three bands at 1136, 1014, and 986 cm^{-1} (Fig. 3), and the two bands at 800 and 736 cm^{-1} correspond to intermediate bending modes between those of O–B–O and O–Be–O. Frost *et al.* (2014) explain these two distinct bands by the occurrence of vibrations involving the two natural isotopes of boron, namely ^{10}B and ^{11}B. However, as underlined by Pekov *et al.* (2010), the band at 736 cm^{-1} could also be assigned to the stretching vibrations of the BeO_4 tetrahedra that generally occur in the 700–800 cm^{-1} range. Finally, the bands below 600 cm^{-1} (571, 550, and 500 cm^{-1}) correspond to lattice vibrations, and the band at 664 cm^{-1} can be assigned to vibrations resulting from the vibrational coupling of Al–O and Be–O stretching modes.

X-Ray Diffraction

The X-ray powder diffraction pattern of touretite was measured with a Rigaku Xcalibur 4-circle diffractometer (Mo$K\alpha$ radiation, EOS CCD detector, camera diameter 40 mm) using a Gandolfi motion (Table 2). Calculated *d* values were obtained from the unit-cell parameter refinement with the LCLSQ software (Burnham 1991), and calculated intensities were obtained from the X-ray powder pattern simulated with the VESTA software (Momma & Izumi 2011), starting from the crystal structure model of touretite (see below). The unit-cell parameters refined from the observed *d* values are $a = 7.315(4)$ Å, $V = 391.4(6)$ $Å^3$.

Single-crystal X-ray diffraction data were obtained using a Rigaku Xcalibur instrument installed at the Department of Earth Sciences at University of Milano. The diffractometer operated at 50kV and 40 mA, with a sample to detector distance of 80 mm and an exposure time of 30 s/frame. Intensity data were corrected for Lorentz-polarization and absorption effects (face-indexed) with the CrysAlis software (Oxford Diffraction 2006). Space group tests lead to the $P\bar{4}3m$ space group, and the refined crystal structure model showed atomic positions for the framework cations and oxygen atoms (Table 4) in good agreement with those of londonite, with which touretite is isostructural (Gatta *et al*. 2010). As in the previous literature for londonite, touretite shows the same behavior with respect to the displacement parameters, with those of the Li/Cs atom almost one order of magnitude larger than those for B and the oxygen atoms. All atoms were refined anisotropically, except B1, O2, and O3 that were "non positive definite" in the first refinement cycles and were subsequently constrained to be isotropic. The final R_1 value is 0.0444 for 226 unique reflections (Table 3, Supplementary data[1]).

TABLE 2. X-RAY POWDER DIFFRACTION DATA FOR TOURETITE (*d* IN Å)

I/I_0	d_{obs}	d_{calc}	I_{calc}	*hkl*
93	7.340	7.315	92	1 0 0
5	3.668	3.657	5	2 0 0
21	3.285	3.271	20	2 1 0
100	2.974	2.986	100	2 1 1
34	2.438	2.438	34	3 0 0
4	2.319	2.313	4	3 1 0
23	2.212	2.206	24	3 1 1
64	2.105	2.112	65	2 2 2
27	1.948	1.955	18	3 2 1
33	1.830	1.829	37	4 0 0
23	1.779	1.774	23	4 1 0
18	1.720	1.724	19	3 3 0
8	1.558	1.560	8	3 3 2
8	1.434	1.435	5	4 3 1
7	1.403	1.408	8	5 1 1
42	1.295	1.293	43	4 4 0
4	1.253	1.255	3	4 3 3
2	1.222	1.219	2	4 4 2

The structure of touretite contains clusters of four edge-sharing AlO_6 octahedra located around the origin of the unit cell and linked to the BeO_4 and BO_4 tetrahedra by corner-sharing with the arrangement shown in Figure 4. The alkali cations occupy the Li/Cs site in a large cavity at the center of the unit cell and have a coordination number of 12. The coordination polyhedron can be described as a truncated tetrahedron (Fig. 5) that shares its small triangular faces with faces of the BeO_4 tetrahedra (Fig. 4).

A mixed Li/Cs occupancy was refined on the 0.5 0.5 0.5 site after constraining 0.18 vacancies *pfu*, leading to

[1] Supplementary Data are available from the Depository of Unpublished Data on the MAC website (http://mineralogicalassociation.ca/), document "Touretite, CM63, 25-00007".

TABLE 3. DETAILS ABOUT THE DATA COLLECTION AND STRUCTURE REFINEMENT OF TOURETITE

Crystal size (μm)	244 × 188 × 149
Crystal color	Pale pink
T (K)	295
Unit-cell parameters	$a = 7.31202(15)$ Å
	$V = 390.942(14)$ Å^3
Simplified formula	$LiAl_4Be_4(B_{11}Be)O_{28}$
Space Group	$P\bar{4}3m$
Z	1
Radiation type	X-ray Mo$K\alpha$
Wavelength (Å)	0.7107
Diffractometer	Rigaku Xcalibur
Data-collection method	ω/φ scan
Step size (°)	1°
θ max. (°)	28.76
hmin, hmax	−9, +9
kmin, kmax	−8, +9
lmin, lmax	−9, +9
no. measured reflections	2878
no. unique reflections	226
no. unique refl. with $I > 2\sigma(I)$	225
no. refined parameters	21
Refinement on	F
Final R_1 (obs/all) (%)	4.44/4.44
Final wR_2 (%)	11.95/11.95
Residuals (e$^-$/ Å^3)	+1.30/−0.54

Note: $R_1 = \Sigma(|F_{obs}-F_{calc}|)/\Sigma|F_{obs}|$; $wR2 = (\Sigma(w(F^2_{obs}-F^2_{calc})^2)/\Sigma(w(F^2_{obs})^2)^{0.5}$, $w = 1/(\sigma^2(F^2_{obs}))$.

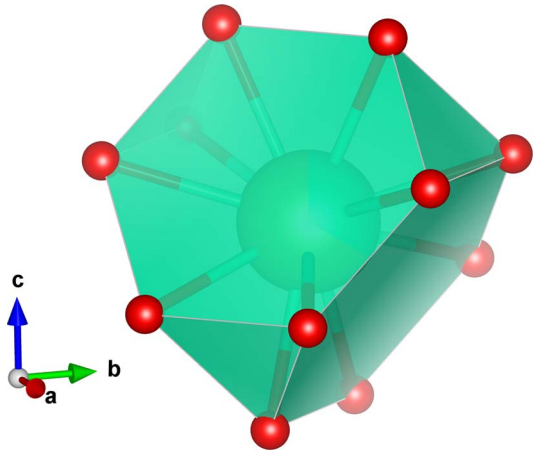

FIG. 5. The large $(Li,Cs)O_{12}$ polyhedron in the crystal structure of touretite showing a morphology of truncated tetrahedron (drawn by VESTA, Momma & Izumi 2011).

0.478(7) Li + 0.342(6) Cs + 0.18 □, in fairly good agreement with the empirical formula calculated from the LA-ICP-TOF-MS analyses (see above). The occupancies of the Be and B sites were constrained to the values calculated from the electron-microprobe data: 0.91 Be/0.09 Li and 0.94 B/0.06 Be, respectively (Table 4). These occupancies are in very good agreement with the observed electron densities, but it was impossible to refine these

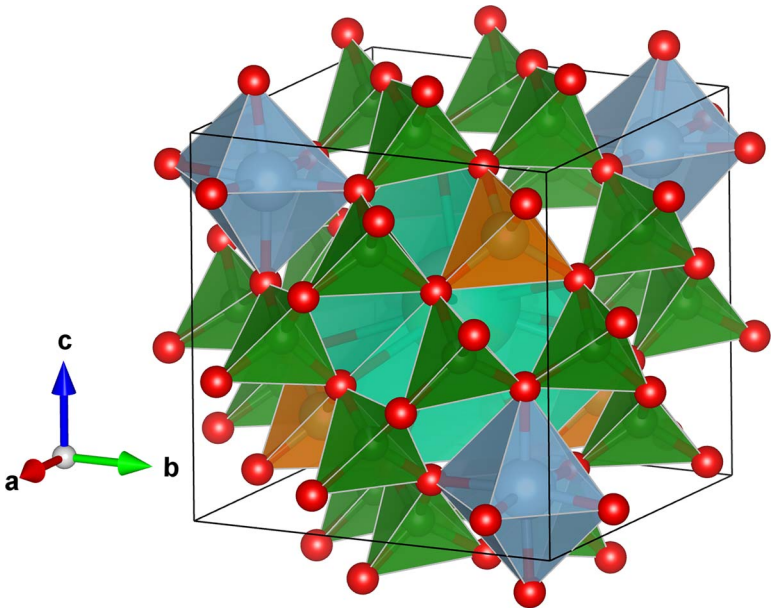

FIG. 4. Clinographic view of the crystal structure of touretite. B-rich (12h) and Be-rich (4e) tetrahedra are shown in green and orange, respectively, and Al (4e) octahedra in blue. The large spheres represent the alkali (1a) site (drawn by VESTA, Momma & Izumi 2011).

TABLE 4. REFINED SITE OCCUPANCIES AND POSITIONAL, ISOTROPIC, AND EQUIVALENT ISOTROPIC DISPLACEMENT PARAMETERS (Å^2) FOR TOURETITE AT 295 K

Site	*x*	*y*	*z*	U_{eq}/U_{iso}[a]
Cs*	1/2	1/2	1/2	0.0327(13)
Al	0.85973(17)	0.14027(17)	0.85973(17)	0.0064(5)
B1**	0.0000	0.5000	0.7497(5)	0.0017(10)[a]
Be2***	0.2415(8)	0.2415(8)	0.7585(8)	0.013(2)
O1	0.1187(4)	0.1187(4)	0.8813(4)	0.0062(12)
O2	0.8630(3)	0.4026(4)	0.8630(3)	0.0025(6)[a]
O3	0.9012(4)	0.6355(3)	0.6355(3)	0.0019(7)[a]

* [0.478(7) Li + 0.342(6) Cs + 0.18 □], ** [0.94 B + 0.06 Be], *** [0.91 Be + 0.09 Li]

occupancies separately due to the very close scattering values for Li, Be, and B.

The best agreement between the Li/Cs site scattering values and the GemTOF data was calculated without considering Rb, Na, and Pb, which occur in very low amounts. The resulting assigned site population is 0.46 Li + 0.29 Cs + 0.18 K + 0.08 □, corresponding to a calculated site scattering value of 20.56 electrons, in good agreement with the 22.24 electrons observed in the structure refinement. The GemTOF data give 0.38 Li + 0.24 Cs + 0.14 K + 0.18 □, but 0.03 Rb, 0.02 Na, and 0.01 Pb also occur at that site. Subtracting these elements and correcting the residual elements to fill the site gives 0.40 Li + 0.26 Cs + 0.15 K + 0.19 □, in very good agreement with the assigned site population, thus confirming the cation occupancies of the large site in the structure.

Selected bond distances and angles of the touretite structure are shown in Table 5. The bond-valence table for touretite, calculated with the empirical parameters of Gagné & Hawthorne (2015), satisfactorily confirms the expected atomic valences for Li/Cs, Al, B, and Be, as well as for O^{2-} at the anion sites (Table 6). A significant under-bonding is observed for the Li/Cs site (0.276 vu), which may be attributed to steric strain resulting from the high site symmetry.

TABLE 5. SELECTED BOND DISTANCES (Å) FOR TOURETITE

Be–O1	1.555(12)	O3–Be–O3 (×3)	113.2(3)
Be–O3 (×3)	1.645(4)	O3–Be–O1 (×3)	105.4(4)
B–O2 (×2)	1.482(3)	O2–B–O3 (×2)	107.8(1)
B–O3 (×2)	1.483(3)	O2–B–O3′ (×2)	108.8(1)
		O2–B–O2	112.1(3)
		O3–B–O3	111.5(3)
Al–O1 (×3)	1.907(3)		
Al–O2 (×3)	1.918(3)		
Cs–O3 (×12)	3.251(3)		

Discussion

Touretite is a borate isostructural with londonite and rhodizite. According to the Strunz classification, the mineral is classified as 06.GC.05 (06 borates, G heptaborates and other megaborates, C tekto-dodecaborates). The Dana number of touretite is 25.08.02.03, and a comparison of the physical properties of touretite with those of londonite and rhodizite is given in Table 7.

Occurrence of lithium in large cavities

Crystal-chemical investigations of lithium minerals show that this element generally occurs in tetrahedral or octahedral coordination polyhedra (Wenger & Armbruster 1991), but an unusual feature of the touretite structure is the presence of lithium in a very large cavity. The possibility of Li occurring in large coordination polyhedra is discussed in detail in the literature for some specific mineral groups. In the alluaudite supergroup of phosphates, Hatert *et al.* (2000, 2002) and Hatert (2004) observed Li substituting for Na in the large channels of the structure, on the 8-fold A(2)' site showing average Li–O distances between 2.71 and 2.84 Å. Deubener *et al.* (1991) synthesized Li-rich feldspars in which lithium also occurs on the large M sites, with an average Li–O bond length of 2.935 Å. Finally, Oberti *et al.* (2003) discuss the substitution of Na by Li in the large M4 sites of the amphibole structure, with average Li–O bond lengths between 2.48 and 2.52 Å.

In this last paper, Oberti *et al*. (2003) explain that, in crystal structures with several cations of different sizes occurring on the same site, the shape of the electron density is very complex. Using a strongly anisotropic model with a single atom, or using a split-atom model, does not change the result: in both cases, the electron densities are difficult to accurately estimate. The very anisotropic displacement ellipsoid, observed on the Cs/Li site in the structure of touretite (Table 4), is certainly produced by this effect. Probably, Li is displaced from the central position in the cavity, toward its borders,

TABLE 6. WEIGHTED BOND-VALENCE VALUES (IN VALENCE UNITS) FOR TOURETITE

	$(Li_{0.38}Cs_{0.24}K_{0.14}Rb_{0.03}Na_{0.02}Pb_{0.01}\square_{0.18})$	$Al_{1.00}$	$(B_{0.94}Be_{0.06})$	$(Be_{0.90}Li_{0.10})$	SUM
O1		0.497 (×3↓×3→)		0.635	2.126
O2		0.482 (×3↓)	0.740 (×2↓→)		1.963
O3	0.046 (×12↓)		0.738 (×2↓→)	0.475 (×3↓)	1.997
SUM	0.554	2.938	2.956	2.060	
Expected	0.830	3.000	2.940	1.900	

to reduce some Li–O bond lengths and, therefore, fulfill its bond-valence requirements.

The structural model of touretite shows an average Al–O distance of 1.913 Å (Table 5), significantly longer than the value 1.904 Å published by Gatta *et al.* (2010). This feature could eventually indicate that lithium also occurs on the Al site of the touretite structure. However, by considering the Shannon (1976) ionic radii, we obtain 0.535 Å for Al[VI] and 1.37 Å for O[III–IV], thus giving a theoretical Al–O distance of 1.905 Å, in fairly good agreement with our value. Even considering only 10% of Li substituting for Al at that site, we would obtain a (Al,Li)–O theoretical bond distance of 1.928 Å (Li[VI] *e.i.r.* = 0.76 Å), much higher than the observed value. Based on our observed bond distances, and assuming full occupancy of the site by Al

TABLE 7. COMPARISON OF THE PHYSICAL PROPERTIES OF TOURETITE, RHODIZITE, AND LONDONITE

Species	Touretite	Rhodizite	Londonite
Reference	This work	[1, 2, 3]	[3]
Ideal formula	$LiAl_4Be_4(B_{11}Be)O_{28}$	$KAl_4Be_4(B_{11}Be)O_{28}$	$CsAl_4Be_4(B_{11}Be)O_{28}$
Space group	$P\bar{4}3m$	$P\bar{4}3m$	$P\bar{4}3m$
a (Å)	7.31202(15)	7.318(1)	7.321(1)
V (Å^3)	390.942(14)	391.90	392.30
Z	1	1	1
Strong X-ray	7.340(93)	7.158(30)	7.342(17)
Lines	3.668(5)	3.633(5)	3.663(10)
	3.285(21)	3.250(35)	3.276(35)
	2.974(100)	2.967(100)	2.990(100)
	-	2.572(5)	-
	2.438(34)	2.428(40)	2.441(50)
	2.319(4)	-	-
	2.212(23)	2.195(45)	2.208(30)
	2.105(64)	2.103(70)	2.113(70)
	1.948(27)	1.957(35)	1.957(35)
	1.830(33)	1.823(50)	1.830(20)
	1.779(23)	1.769(40)	1.776(40)
	1.720(18)	1.719(25)	1.726(15)
	1.558(8)	1.555(10)	1.561(5)
	1.434(8)	1.431(15)	1.436(10)
	1.403(7)	1.405(10)	1.409(8)
	1.295(42)	1.291(45)	1.294(20)
Morphology	{110}, rare {111}{$\bar{1}$11}	{110}, rare {221}{211}{111}, very rare{100}	{110}, rare {221}{211}{111}, very rare{100}
Cleavage	None	None	None
Fracture	Conchoidal	Conchoidal	Conchoidal
Density	3.06(meas.)	3.36(meas.)	3.34(meas.)
Refraction index	1.608	1.690	1.693
Hardness	8	8	8
Colour	White to pale pink	White, yellow, greenish	White to yellow

[1] Pring *et al.* (1986), [2] Laurs *et al.* (2002), [3] Simmons *et al.* (2001)

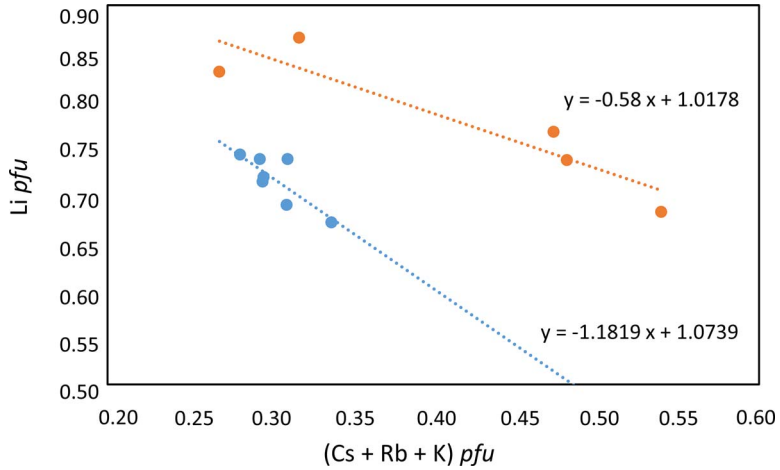

FIG. 6. Correlations between the Li and (Cs + Rb + K) contents (*pfu*) of touretite. The blue line and dots correspond to the data collected by the AKNŠZ research team, while the red line and dots correspond to the data obtained by the HPV team.

and Li, we obtain a maximum amount of 3.5% Li, so we can reasonably assume that the occurrence of Li on the Al site of londonite is not significant, and that most Li is localized on the Li/Cs and on the Be sites.

Bond-valence sums on the Al site, calculated as 2.938 (Table 6), are also close to the ideal value corresponding to a full Al occupancy. By considering three longer bonds of Al with O3, this bond-valence sum is further increased to 3.06 *v.u.*, thus further indicating that the presence of minor Li on the Al site is highly unlikely.

Substitution mechanisms

Touretite was investigated independently by two groups of researchers, and both teams arrived at the same conclusions about the crystallography and the chemical composition of the species. We decided to merge the research teams and to keep most data of Frédéric Hatert and co-workers; nevertheless, the chemical data obtained by Radek Škoda on another crystal from the same locality are very interesting and allowed us to establish several correlations discussed below.

As shown in Figure 6, good negative correlations exist between Li *pfu* and (Cs+Rb+K) *pfu*, thus confirming the presence of Li on the large site of the structure. For the crystal of the AKNŠZ research team, the correlation shows a slope close to −1 (Fig. 6), thus indicating a simple homovalent substitution mechanism $Li^{+} = (Cs + Rb + K)^{+}$. For the sample of the HPV team, the situation is more complex, since the slope is close to −0.6 (Fig. 6). This is certainly due to the fact that, in this sample, Li occurs in larger amounts, because it is also present at the Be site.

Examination of the empirical formula of this sample (see above) shows that 0.4 Li replaces beryllium at the Be site, and that 0.28 B replaces beryllium at the B site (normally occupied by 11B and 1Be *pfu*). The incorporation of Li at the Be site can, therefore, be explained by the coupled heterovalent substitution mechanism: $Be^{2+} + Be^{2+} = Li^{+} + B^{3+}$.

Factors controlling the formation of touretite

During their formation, pegmatite deposits are affected by a fractional crystallization process that induces geochemical variations reflected in the chemical composition of mineral species; this fractionation consequently provokes increases of the Mn/Fe, Ta/Nb, Hf/Zr, Rb/K, and Cs/Li ratios (Simmons *et al.* 2004). In the most evolved pegmatites, zircon is enriched in Hf, iron-manganese phosphates are enriched in Mn, and alkali feldspars are enriched in Rb, while oxides of the columbite group become Ta- and Mn-rich and evolve toward tantalite-(Mn).

The crystallization of lithium-rich species is certainly the most prominent sign of fractionation, with the formation of elbaite, "lepidolite", spodumene, petalite, and phosphates of the triphylite–lithiophilite and amblygonite–montebrasite series. Cs-rich species only occur in highly fractionated pegmatites, where pollucite and pezzottaite appear.

Minerals of the rhodizite group certainly occupy a special position in these genetic sequences. Due to the large cavity in their crystal structure, they are able to accommodate alkalis such as K, Cs, and Rb, as well as the smaller Li atom. Therefore, they can be used as a probe to decipher the evolution of both the Rb/K and Cs/Li ratio. Simmons *et al.* (2001) underlined that, in the Betafo mining district, Cs-rich londonite

is observed in the most evolved pegmatites, occurring in the northwestern part of the district, while Cs-poor and K-rich rhodizite samples occur in the less evolved deposits at the eastern part of the district. The geographic position of Ambalabe, where touretite samples were found, corresponds to the eastern part of the Betafo district, where less evolved Cs-poor pegmatites occur. This feature explains why the Cs-content of touretite is relatively low.

Mineral species in close association with touretite include Li-rich tourmaline-group minerals, "lepidolite", and spodumene, thus indicating that the Ambalabe pegmatite is moderately fractionated, with Li-rich species but without Cs-rich species as pezzottaite or pollucite. As a consequence, londonite, touretite, and rhodizite certainly constitute good indicators of highly, moderately, and poorly fractionated pegmatite deposits, respectively. This rule, however, cannot be strictly applied, since minerals of the rhodizite group generally occur in miarolitic cavities where late fluid circulations may affect their geochemistry.

Conclusions

Pegmatites of Madagascar are well known for their gorgeous gem minerals that mostly form authigenic crystals in miarolitic cavities. This unique feature, associated with the high fractionation degree of the deposits, is responsible for the crystallization of rare gemstones as, for example, pezzottaite, a Cs-rich mineral of the beryl group (Laurs *et al*. 2003), which is one of the few recently described mineral species mined as valuable gem material.

Borates of the rhodizite–londonite series also belong to this category of rare gems from Madagascar (Laurs *et al*. 2002), and we may expect, in the future, to see gem-quality touretite appearing on the international gem market. Moreover, the occurrence of significant amounts of Rb on the large alkali site of the structure, as well as the presence of vacancies, incite us to pursue the study of this mineral group, in which, for sure, potential new mineral species are still to be found.

Acknowledgments

This work was done with the support of the Russian Science Foundation grant 24-27-00225 for Atali A. Agakhanov. Many thanks are due to Dr. Anthony R. Kampf, as well as to an anonymous reviewer, for their constructive comments.

References

Burnham, C.W. (1991) *LCLSQ version 8.4, Least-Squares Refinement of Crystallographic Lattice Parameters*. Harvard University Department of Earth and Planetary Sciences, Cambridge, Massachusetts, USA (24 pg.).

Černý, P. & Ercit, T.S. (2005) The classification of granitic pegmatites revisited. *The Canadian Mineralogist* **43**, 2005–2026.

Damour, A. (1882) Sur la rhodizite. *Bulletin de la Société française de Minéralogie et de Cristallographie* **5**, 98–103 (in French).

Deubener, J., Sternitzke, M., & Müller, G. (1991) Feldspars $MAlSi_3O_8$ (M = H, Li, Ag) synthesized by low-temperature ion exchange. *American Mineralogist* **76**, 1620–1627.

Frost, R.L., López, A., Xi, Y., Scholz, R., Souza, L., & Lana, C. (2014) The molecular structure of the borate mineral rhodizite $(K,Cs)Al_4Be_4(B,Be)_{12}O_{28}$–A vibrational spectroscopic study. *Spectrochimica Acta* **A128**, 291–294.

Gagné, O.C. & Hawthorne, F.C. (2015) Comprehensive derivation of bond-valence parameters for ion pairs involving oxygen. *Acta Crystallographica* **B71**, 562–578.

Gatta, G.D., Vignola, P., Mcintyre, G.J., & Diella, V. (2010) On the crystal chemistry of londonite [$(Cs,K,Rb)Al_4Be_5B_{11}O_{28}$]: A single-crystal neutron diffraction study at 300 and 20 K. *American Mineralogist* **95**, 1467–1472.

Gatta, G.D., Vignola, P., & Yongjae, L. (2011) Stability of $(Cs,K)Al_4Be_5B_{11}O_{28}$ (londonite) at high pressure and high temperature: A potential neutron absorber material. *Physics and Chemistry of Minerals* **38**, 429–434.

Hatert, F. (2004) The crystal chemistry of lithium in the alluaudite structure: A study of the $(Na_{1-x}Li_x)_{1.5}Mn_{1.5}Fe^{3+}_{1.5}(PO_4)_3$ solid solution (x = 0 to 1). *Mineralogy and Petrology* **81**, 205–217.

Hatert, F., Keller, P., Lissner, F., Antenucci, D., & Fransolet, A.-M. (2000) First experimental evidence of alluaudite-like phosphates with high Li-content: The $(Na_{1-x}Li_x)MnFe_2(PO_4)_3$ series (x = 0 to 1). *European Journal of Mineralogy* **12**, 847–857.

Hatert, F., Antenucci, D., Fransolet, A.-M., & Liegeois-Duyckaerts, M. (2002) The crystal chemistry of lithium in the alluaudite structure: A study of the $(Na_{1-x}Li_x)CdIn_2(PO_4)_3$ solid solution (x = 0 to 1). *Journal of Solid State Chemistry* **163**, 194–201.

Hofmeister, A.M., Hoering, T.C., & Virgo, D. (1987) Vibrational spectroscopy of beryllium aluminosilicates: Heat capacity calculations from band assignments. *Physics and Chemistry of Minerals* **14**, 205–224.

Kim, C.C., Bell, M.I., & McKeown, D.A. (1995) Vibrational analysis of beryl $(Be_3Al_2Si_6O_{18})$ and its constituent ring (Si_6O_{18}). *Physica B: Condensed Matter* **205**(2), 193–208.

Lacroix, A. (1922) *Minéralogie de Madagascar*, *vol. 1*. Editions Augustin Challamel, Paris, France (in French).

Laurs, B.M., Pezzotta, F., Simmons, W.B., Falster, A.U., & Muhmeister, M. (2002) Rhodizite-londonite from the Antsongombato pegmatite, Central Madagascar. *Gems and Gemology* **38**, 326–339.

Laurs, B.M., Rossman, G.R., Quinn, E.P., McClure, S.F., Peretti, A., Armbruster, T., Hawthorne, F.C., Falster, A.U., Günther, D., Cooper, M.A., & Grobéty, B. (2003) Pezzottaite from Ambatovita, Madagascar: A new gem mineral. *Gems and Gemology* **39**, 284–301.

Mandarino, J.A. (1981) The Gladstone-Dale relationship: Part IV. The compatibility concept and its application. *Canadian Mineralogist* **19**, 441–450.

Momma, K. & Izumi, F. (2011) VESTA 3 for three-dimensional visualization of crystal, volumetric and morphology data. *Journal of Applied Crystallography* **44**, 1272–1276.

Oberti, R., Cámara, F., Ottolini, L., & Caballero, J.M. (2003) Lithium in amphiboles: Detection, quantification, and incorporation mechanisms in the compositional space bridging sodic and ^{B}Li-amphiboles. *European Journal of Mineralogy* **15**, 309–319.

Oxford Diffraction (2006) *Crys Alis PRO*. Oxford Diffraction Ltd., Abingdon, Oxfordshire, United Kingdom.

Pekov, I.V., Yakubovich, O.V., Massa, W., Chukanov, N.V., Kononkova, N.N., Agakhanov, A.A., & Karpenko, V.Y. (2010) Londonite from the Urals, and new aspects of the crystal chemistry of the rhodizite-londonite series. *Canadian Mineralogist* **48**, 241–254.

Pezzotta, F. (2001) Madagascar – A Mineral and Gemstone Paradise No. 1. Lapis International, Tucson, Arizona, USA (97 pg.).

Pezzotta, F. (2005) First attempt to the petrogenesis and classification of granitic pegmatites of the Itremo Region (Madagascar). Proceedings of the Crystallization Processes in Granitic Pegmatites International Meeting, May 23rd–29th, 2005, Elba Island, Italy.

Pring, A., Din, V.K., Jefferson, D.A., & Thomas, J.M. (1986) The crystal chemistry of rhodizite: A re-examination. *Mineralogical Magazine* **50**, 163–172.

Rose, G. (1834) Über den Rhodizit, eine neue Mineralgattung. *Annalen der Physik und Chemie Poggendorff* **33**, 253–256 (in German).

Ross, S.D. (1972) The vibrational spectra of some minerals containing tetrahedrally co-ordinated boron. *Spectrochimica Acta* **A28**(8), 1555–1561.

Shannon, R.D. (1976) Revised effective ionic radii and systematic studies of interatomic distances in halides and chalcogenides. *Acta Crystallographica* **A32**, 751.

Simmons, W.B., Pezzotta, F., Falster, A.U., & Webber, K.L. (2001) Londonite, a new mineral species: The Cs-dominant analogue of rhodizite from the Antandrokomby pegmatite, Madagascar. *The Canadian Mineralogist* **39**, 747–755.

Simmons, W.B., Webber, K.L., Falster, A.U., & Nizamoff, J.W. (2004) *Pegmatology: Pegmatite Mineralogy, Petrology and Petrogenesis*. Rubellite Press, New Orleans, Louisiana, USA (176 pg.).

Totaro, K. (2021) *Etude Cristallochimique d'Échantillons de Londonite et de Rhodizite des Pegmatites de Madagascar*. Unpublished MSc thesis. University of Liège, Liège, Belgium (97 pg.).

Wang, H.A.O. & Krzemnicki, M.S. (2021) Multi-element analysis of minerals using laser ablation inductively coupled plasma time of flight mass spectrometry and geochemical data visualization using t-distributed stochastic neighbor embedding: Case study on emeralds. *Journal of Analytical Atomic Spectrometry* **36**(3), 518–527.

Warr, L.N. (2021) IMA-CNMNC approved mineral symbols. *Mineralogical Magazine* **85**, 291–320.

Wenger, M. & Armbruster, T. (1991) Crystal chemistry of lithium: Oxygen coordination and bonding. *European Journal of Mineralogy* **3**, 387–399.

Received January 15, 2025. Revised manuscript accepted July 14, 2025.

This manuscript was handled by Guest Editor Jon Errandonea and Editor Stephen Prevec.